

Reconstruction of Bandlimited Periodic Nonuniformly Sampled Signals through Multirate Filter Banks

Ryan S. Prendergast, *Student Member, IEEE*, Bernard C. Levy, *Fellow, IEEE*, and Paul J. Hurst, *Fellow, IEEE*

Abstract—A bandlimited signal can be recovered from its periodic nonuniformly spaced samples provided the average sampling rate is at least the Nyquist rate. A multirate filter bank structure is used to both model this nonuniform sampling (through the analysis bank) and reconstruct a uniformly sampled sequence (through the synthesis bank). Several techniques for modelling the nonuniform sampling are presented for various cases of sampling. Conditions on the filter bank structure are used to accurately reconstruct uniform samples of the input signal at the Nyquist rate. Several examples and simulation results are presented, with emphasis on forms of nonuniform sampling that may be useful in mixed-signal integrated circuits.

Index Terms—Bunched sampling, multirate signal processing, nonuniform sampling, time-interleaved analog-to-digital converters.

I. INTRODUCTION

IT HAS been known for some time that a bandlimited signal can be completely reconstructed from discrete samples. Early work of Nyquist [1] served to recognize the maximum allowable sampling interval, later dubbed the “Nyquist interval,” which retains complete signal information. Thus, it is not surprising that the most basic form of sampling, the uniform sampling theorem, had been well established within the field prior to its inclusion in Shannon’s classic paper roughly two decades later [2]. Alternative sampling techniques are only slightly more modern, with Shannon introducing the idea of derivative sampling in his same classic paper. Additional early work [3] examined several different classes of nonuniform sampling including the case of periodic nonuniform sampling. Such periodic cases, including Shannon’s derivative sampling, fall under the generalized sampling expansion (GSE) of Papoulis [4], which shows that a bandlimited signal passed through L distinct linear time-invariant systems can be reconstructed from the L outputs uniformly sampled at a minimum of $1/L^{th}$ the Nyquist rate. Subsequent support of the GSE with further analysis was established in [5]. These past works

provide a foundation for the development of realizable periodic nonuniform sampling schemes.

More recently, several techniques have been introduced which rely on multirate filter banks to reconstruct a continuous-time or uniformly sampled discrete-time signal from its periodic nonuniform samples. Initial application of multirate filter banks for generalized sampling purposes, including nonuniform sampling, was presented in [6]. Follow up work by the same authors [7] established a more reliable method of determining a discrete-time filter bank for reconstruction of a signal from its nonuniform samples. A technique based on a continuous-time reconstruction filter bank, along with a method for conversion to discrete-time, was developed in [8]. Discrete-time fractional delay filters were employed in a filter bank structure [9] to reconstruct a class of oversampled signals. One formulation [10] viewed the design of the reconstruction filters as a communications equalization problem through a least-squares solution. The multirate filter bank structure was also used in [11], [12] to employ a nonuniform technique for optimal sampling of multiband signals.

Alternate reconstruction methods that do not use a filter bank structure exist for various classes of nonuniformly sampled signals. In cases where the sampling pattern is non-periodic, the filter bank structure cannot be applied as in the periodic case. Techniques for the recovery of non-periodically sampled signals are typically more computationally complex than a filter bank, and often require iterative methods. An example alternate technique developed for the periodic case is [13], which recovers the spectral content of a uniformly sampled signal based on points in the nonuniformly sampled spectrum. Requiring a matrix multiplication for each spectral point recovered, the computational cost is considerably greater than recovery through a filter bank. This paper will deal only with the subclass of periodically sampled signals, and a multirate filter bank structure will be used for recovery. The broader class of nonuniformly sampled signals along with applications is examined in [14].

This paper presents a purely discrete-time filter bank implementation for reconstruction of a periodic nonuniformly sampled signal. While comparable in structure to previous methods, a new technique has been developed for determining the reconstruction filter bank. Reconstruction filters are finite-impulse response (FIR), guaranteeing a realizable system. As mentioned above, this implementation is only applicable to cases where the sampling is periodic.

Manuscript received March 20, 2003; revised January 31, 2004. This research has been supported by NSF Grant ECS-0121469 and UC Micro Grant 01-084. The associate editor coordinating the review of this paper and approving it for publication was Dr. Antonio Petraglia.

R. S. Prendergast was with the University of California at Davis, Davis, CA 95616 USA. He is now with the Department of Electrical and Computer Engineering, University of California at San Diego, La Jolla, CA 92093 USA (e-mail: rprender@ucsd.edu).

B. C. Levy and P. J. Hurst are with the Department of Electrical and Computer Engineering, University of California at Davis, Davis, CA 95616 USA (e-mail: levy@ece.ucdavis.edu; hurst@ece.ucdavis.edu).

The paper organization is as follows. Specific motivation for the paper is discussed in Section II, focusing on two particular applications for periodic nonuniform sampling: bunched sampling and time-interleaved samplers. Signal modelling and the design of reconstruction filters are presented in Section III. An extension of the techniques to cases of oversampling is presented in Section IV. Examples with simulation results are presented in Section V, along with comments on performance as related to prior methods. Finally, Section VI provides concluding remarks.

II. APPLICATIONS

Motivation for a practical reconstruction scheme has come mainly from the area of analog-to-digital converters (ADCs). Correction of small periodic timing errors in a time-interleaved ADC was the motivation in [9], [10], [13]. Earlier work by the authors of this paper [15] developed a solution for a simple case of bunched sampling for the purpose of noise reduction in mixed-signal integrated circuits (ICs). The solution developed in this paper will be applied to both of these cases.

A. Time-Interleaved ADCs

Application to a time-interleaved ADC, as depicted in Fig. 1, will be discussed first. A standard ADC uniformly samples an analog continuous-time signal and subsequently converts the discrete-time samples into a digital signal through quantization. The quantized signal is then processed by a digital signal processor (DSP). If the L parallel ADCs in Fig. 1 each operate at rate f_s/L , their sampling instants can be spaced to obtain the samples that a single ADC sampling at f_s would obtain. The L streams of ADC output are multiplexed together such that the digital output signal can be operated on by a DSP using standard methods. Slight skews in the sample times of the individual ADCs can result in a periodic nonuniformly sampled output after combination.

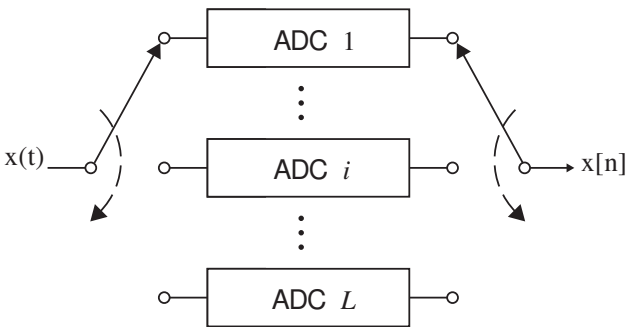


Fig. 1. L -branch time-interleaved ADC, converting a continuous-time signal $x(t)$ to the discrete-time signal $x[n]$. Each converter operates at $1/L^{th}$ the sampling rate of $x[n]$.

B. Noise Reduction in a Mixed Signal IC

A mixed-signal IC contains both digital-signal-processing and analog circuits, often in the form of an analog front end, which includes an ADC, followed by a DSP. Switching in the DSP generates noise that can couple into the analog signal path

through parasitic signal paths [16], [17], corrupting the analog signal and reducing the signal-to-noise ratio. Techniques for reducing such noise coupling exist, e.g., the physical separation of analog and digital portions to attenuate the interference.

Another technique is to separate the DSP and analog processing in time through use of a bunched (nonuniform) sampling pattern. Operation of the circuit is divided into two separate phases, sampling and processing. During the first phase, the sampling phase, the analog signal is sampled at a fast rate while the DSP circuits are off and not processing, and hence are not generating noise. During the second phase, the processing phase, the DSP is allowed to run at full capacity and the analog signal is not sampled by the ADC. By alternating between these two phases, samples of the analog signal are obtained but digital noise coupling to the analog signal is avoided during the sampling times.

This two-phase method of operation can be employed in ICs processing a bandlimited signal provided the average ADC sampling rate is at least the Nyquist rate (meeting the GSE criteria of [4]). The bunched samples can then be converted to uniform samples as is illustrated in Fig. 2(a), and the uniform samples can be subsequently processed using standard DSP techniques. The reconstruction technique discussed in this paper recovers the uniformly spaced samples at the Nyquist rate, $\hat{x}[n]$, from the bunched ADC output, $x_b[n]$, as shown in Fig. 2(b).

III. DESIGN OF RECONSTRUCTION FILTER BANK

This section will present the analysis and design of a filter bank that accurately reconstructs uniform samples from the periodic nonuniform samples of a bandlimited signal. This filter bank will be applied to both the bunched sampling and interleaved sampling applications described in the previous section.

Throughout this section a continuous-time signal, $x(t)$, with bandwidth β radians/sec will be considered. By definition, this signal's continuous-time Fourier transform, $X(j\Omega)$, is equal to zero for all $|\Omega| > \beta$. Uniform sampling at rate $f_s = 1/T_s$ would produce the discrete-time signal given by $x[n] = x(nT_s)$. The discrete-time Fourier transform of $x[n]$ is given by

$$X(e^{j\omega}) = \frac{1}{T_s} \sum_{k=-\infty}^{\infty} X \left[j \left(\omega - \frac{2\pi k}{T_s} \right) \right] \Big|_{\Omega=\omega/T_s}, \quad (1)$$

and, provided the sampling period is no greater than the Nyquist period, or $T_s \leq T_N = \pi/\beta$, there will be no aliasing. As (1) is periodic, this paper will only consider the frequency range $|\omega| \leq \pi$, using the normalized frequency convention where sampling rate $\omega_s = 2\pi$.

The generalized multirate filter bank structure for periodic nonuniform sampling reconstruction is shown in Fig. 3. Samples of the discrete-time input signal, $x[n]$, are uniformly taken by each of the L channels in the analysis bank. This model allows for any sampling pattern which is periodic with period MT_s and contains L samples per period.

The analysis bank of Fig. 3 models the periodic sampling process with delays d_i and M -fold decimation operations. It

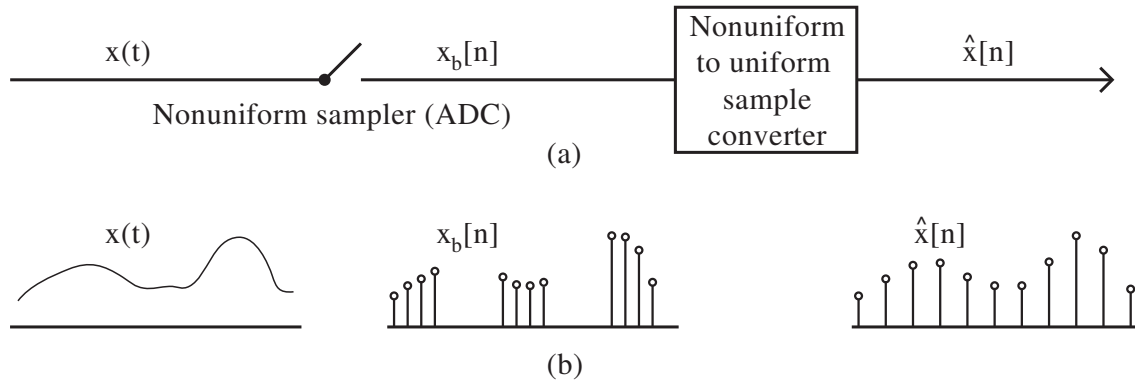


Fig. 2. (a) Proposed method for nonuniform sampling and subsequent conversion to Nyquist-rate uniform samples and (b) corresponding signals.

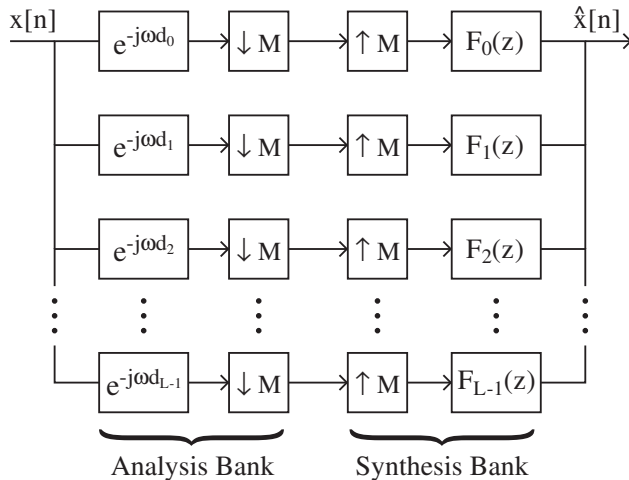


Fig. 3. Generalized filter bank structure for periodic nonuniform sampling, with L channels and common decimation and expansion factor, M .

serves to split $x[n]$ into L signals, each sampled at $1/M^{\text{th}}$ the rate of $x[n]$. As the analysis filters are only delays, each of these L signals can be obtained from sampling a delayed $x(t)$ at a rate of $f_s/M = 1/MT_s$. In actual implementation, the analysis bank does not exist. It is used in Fig. 3 as a discrete-time model for whichever ADC method is used to acquire the samples of $x(t)$. An accurate discrete-time model will be necessary for effective reconstruction. It should be mentioned that since a discrete-time model is being considered, the frequency domain representations of the analysis filter delays will generally only be valid for $|\omega| \leq \pi$ (the same applies to fractional delay terms throughout the paper). This portion of the spectrum is sufficient to completely describe the discrete-time delay, since it is periodic with period 2π .

Reconstruction is performed through the other half of Fig. 3, the synthesis bank, which is composed of M -fold expansion operations and filters $F_0(z), F_1(z), \dots, F_{L-1}(z)$. Each channel of the filter bank has its sampling rate increased. The resulting signal is filtered by a synthesis filter, and then all filter outputs are combined to produce $\hat{x}[n]$. The synthesis filters are to be designed such that $\hat{x}[n]$ is a delayed version of the input $x[n]$; that is, they correct for the aliasing and distortion induced by the nonuniform sampling process,

modelled by the analysis bank. While the output is a discrete-time signal, its continuous-time equivalent can be recovered using a continuous-time lowpass filter with bandwidth β . The advantage of recovering a discrete version of the signal is that an all digital implementation can be employed.

A. Model Analysis Bank

The analysis bank is used to provide a discrete-time model for the actual periodic sampling. The eventual goal is to determine synthesis filters which adequately complement the analysis filters, such that there is little error between the ideal uniformly sampled sequence, $x[n]$, and the reconstructed sequence, $\hat{x}[n]$. As the entire analysis bank only models the sampled signal, it will often be referred to as the “model analysis bank” and its filters as “model analysis filters.”

The continuous-time analysis bank model for periodic nonuniform sample acquisition is shown in Fig. 4. This model contains L delayed and sampled versions of the input continuous-time signal, $x(t)$. Each sampler, operating at rate f_s/M , produces the discrete-time output subsequence

$$x_i[n] = x(nMT_s - \Delta_i), \quad (2)$$

for $i = 0, 1, \dots, L-1$, where the Δ_i are the delay terms. The output of the i^{th} sampler is the input to the expander in the i^{th} channel of the filter bank in Fig. 3. As there are L samplers each operating at rate f_s/M , the average sampling rate is Lf_s/M . As this value must be greater than or equal to the Nyquist rate, the individual samplers must operate at

$$f_s/M \geq f_N/L. \quad (3)$$

This continuous-time analysis bank model can easily be transformed into a discrete-time model of the type shown in Fig. 3. The discrete-time input signal, $x[n]$, has a sampling rate of f_s , or M times that of the subsequences in (2). Thus, the M -fold decimators can replace the slow samplers in Fig. 4. The discrete-time delays can be found from the continuous-time delays through $d_i = \Delta_i/T_s$. These delay terms can be viewed as simple filters,

$$H_i(e^{j\omega}) = e^{-j\omega d_i}, \quad (4)$$

which have the inverse Fourier transform of

$$h_i[n] = \text{sinc}(\pi(n - d_i)) = \frac{\sin(\pi(n - d_i))}{\pi(n - d_i)}. \quad (5)$$

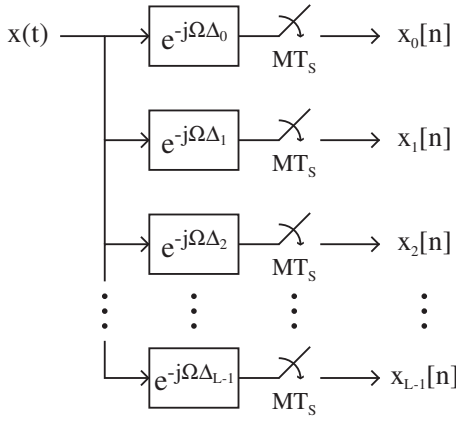


Fig. 4. Continuous-time model analysis bank for periodic nonuniform sampling.

This discrete-time response is of infinite length (provided d_i is not an integer) but decays as $|n - d_i|$ grows large. The subsequences of (2) can thus be written as

$$x_i[n] = (h_i[n] * x[n]) \downarrow M, \quad (6)$$

where $*$ denotes discrete-time convolution and $\downarrow M$ denotes the M -fold decimation operation which retains only samples with indexes divisible by M . In the case of d_i being integer, (5) reduces to a d_i tap delay allowing for a much simpler filter. These single tap delays can be modelled exactly using a finite representation, unlike the infinite length representations required to precisely model analysis filters not corresponding to an integer d_i . Because of this, a model analysis bank with a greater number of integer d_i is more desirable than a model with fewer.

Practically, the relative differences between the continuous delays, Δ_i , are considerably more important than the exact delay values. This is because a common delay term can always be added onto all samplers with no change in the recovered signal output other than a corresponding delay. It is only for notational convenience that $t = 0$ is assigned to a particular moment. As such, a common term can be added to or removed from the d_i . This allows at least one d_i to be an integer, even in cases where sample timing error prohibits precise selection of Δ_i relative to one another. In cases where the Δ_i can be selected under particular constraints, they should be selected to maximize the number of resulting integer d_i , which corresponds to having as many Δ_i spaced by multiples of T_s as possible.

Some final modifications must be made to the analysis filters given in (5), as the numerical solution that will be used to determine the FIR synthesis filters requires FIR analysis filters. Unfortunately, the ideal modelling of (5) will generally require an infinite number of nonzero coefficients. Because of this, finite length models that closely approximate the delays of (4) are necessary. Some error will result from these approximations, but they can be kept sufficiently small such that the reconstruction solution is accurate.

To approximate the delays with a finite number of coefficients, the natural choice is to truncate the model filter (5)

about d_i since the ideal $h_i[n]$ decays as $|n - d_i|$ increases. Further, a windowing function, $q_i[n]$, is also used which produces FIR model analysis filters according to

$$h_i[n] = \begin{cases} \text{sinc}(\pi(n - d_i))q_i[n] & \text{for } |n - d_i| \leq m \\ 0 & \text{for } |n - d_i| > m. \end{cases} \quad (7)$$

This windowed filter will be of length $2m$ unless d_i is an integer, in which case it is trivial. The windowing function serves to smooth the time response. Without this windowing a truncated filter's magnitude response is subject to Gibbs phenomenon, or large amounts of ripple. Frequency domain convolution serves to smooth out the ripple effects, although at the expense of an increased region of transition. A large variety of windows exist and all are subject to some form of a tradeoff between increased transition region and smoothing capabilities [18]. To account for the possibly fractional delay d_i , standard window design techniques may require some modification to provide the same fractional delay as discussed in [19]. This paper considers the Kaiser window, which has the design feature that the tradeoff between its transition region width and smoothing capability is somewhat controllable through its parameter β .

For the model filters of (7), the transition region takes the form of a small region of magnitude response inaccuracy centered about $\omega = \pi$. This makes the analysis bank a poor model for signals occupying these frequencies. Higher order analysis filters will reduce the region of this error, as will decreasing the transition region through window design. The use of higher order filters can only go so far; eventually the need for a simple model outweighs the diminishing gain in performance (and as will be shown, reconstruction filter complexity increases with model filter complexity). Decreasing the transition region through windowing parameters is also of limited use due to the increase in undesirable ripple effects throughout a large portion of the spectrum, resulting in an inaccurate model. While this tradeoff is acceptable for some applications, it is not for this case of signal modelling as even slight errors in modelling can produce large errors in reconstruction. As such, the presence of a transition region around $\omega = \pi$ is tolerated and avoided by oversampling the bandlimited signal such that its normalized spectrum is zero for the transition region. Such circumvention of the transition region is sufficient for this situation. Decreasing the transition region is, however, always desirable as it reduces the required average sampling rate for a given bandlimited signal.

B. Formation of FIR Synthesis Filters

To clearly illustrate the technique for determining FIR reconstruction filters, the following discussion will assume that $L = M$ and that $x[n]$ occupies the entire normal spectrum. These assumptions are equivalent to stating that the sampling rate of $x(t)$ equals the Nyquist rate and the sampling pattern is periodic with period LT_s .

The analysis filters given by (7) can be represented in

polyphase matrix form as

$$\begin{bmatrix} H_0(z) \\ \vdots \\ H_{L-1}(z) \end{bmatrix} = \mathbf{E}(z^L) \begin{bmatrix} 1 \\ \vdots \\ z^{-(L-1)} \end{bmatrix}, \quad (8)$$

using the type-one polyphase matrix,

$$\mathbf{E}(z) = \begin{bmatrix} E_{0,0}(z) & \dots & E_{0,L-1}(z) \\ \vdots & \ddots & \vdots \\ E_{L-1,0}(z) & \dots & E_{L-1,L-1}(z) \end{bmatrix}. \quad (9)$$

Similarly, the synthesis bank is given by

$$\begin{bmatrix} F_0(z) & \dots & F_{L-1}(z) \end{bmatrix} = \begin{bmatrix} z^{-(L-1)} & \dots & 1 \end{bmatrix} \mathbf{R}(z^L), \quad (10)$$

where the type-two polyphase matrix takes the form

$$\mathbf{R}(z) = \begin{bmatrix} R_{0,0}(z) & \dots & R_{0,L-1}(z) \\ \vdots & \ddots & \vdots \\ R_{L-1,0}(z) & \dots & R_{L-1,L-1}(z) \end{bmatrix}. \quad (11)$$

For the application of sampling reconstruction, it is desired for the output, $\hat{x}[n]$, to equal the input, $x[n]$, or at least a scaled and delayed version of the input. This is referred to as the perfect reconstruction (PR) condition, and is achieved if

$$\hat{x}[n] = cx[n-d], \quad (12)$$

for some nonzero scaling value c and integer delay d . An equivalent condition is

$$\hat{X}(z) = cz^{-d}X(z). \quad (13)$$

Errors in the output signal which prevent perfect reconstruction take the form of amplitude distortions, phase distortions, and the presence of aliasing components. As shown in [20], a maximally decimated filter bank is a perfect reconstruction system if $\mathbf{P}(z)$, the product of the synthesis and analysis polyphase matrices which are respectively given by (11) and (9), satisfies

$$\mathbf{P}(z) = \mathbf{R}(z)\mathbf{E}(z) = cz^{-d} \begin{bmatrix} \mathbf{0} & \mathbf{I}_{L-r} \\ z^{-1}\mathbf{I}_r & \mathbf{0} \end{bmatrix}, \quad (14)$$

where \mathbf{I}_α denotes the $\alpha \times \alpha$ identity matrix and where the overall system delay of (13) is determined through $d = Ld' + r + (L-1)$. As $\mathbf{E}(z)$ is known in this situation, the polyphase matrix of the synthesis bank is given by,

$$\mathbf{R}(z) = \mathbf{P}(z)\mathbf{E}^{-1}(z), \quad (15)$$

and the individual synthesis filters are determined through (10).

The solution of (15) requires the inversion of a polynomial matrix, which can be problematic. First, for an inverse to exist, $\mathbf{E}(z)$ must be nonsingular, or of full rank. In relation to the case of periodic sampling, this requires that all delay terms, Δ_i in (2), be distinct. Additionally, the difference between two different Δ_i cannot be a multiple of MT_s (a case where one sampler produces a delayed copy of the sequence another sampler produces). Selection of a nonsingular $\mathbf{E}(z)$ is fairly simple in practice.

A nonsingular $\mathbf{E}(z)$ has an inverse given by

$$\mathbf{E}^{-1}(z) = \frac{\text{adj}(\mathbf{E}(z))}{\det(\mathbf{E}(z))}, \quad (16)$$

where $\text{adj}(\cdot)$ refers to the adjoint operation and $\det(\cdot)$ refers to the determinant operation. Except in very specific cases of cancellation (which will not occur in these nonuniform sampling applications), the individual polynomial elements of $\mathbf{E}^{-1}(z)$ will be infinite-impulse response (IIR) due to the $\det(\mathbf{E}(z))$ denominator term. This term is common to all elements of $\mathbf{E}^{-1}(z)$ and its roots determine the poles of the synthesis filter transfer functions. The poles can exist inside, on, or outside the unit circle. Stable causal transfer functions can be determined for the poles inside the unit circle. Likewise, stable anticausal transfer functions can be found for the poles outside the unit circle. The poles which exist on the unit circle produce transfer functions which are unstable. If $\det(\mathbf{E}(z))$ has such roots on the unit circle, $\mathbf{E}(z)$ will be singular for frequencies corresponding to the unit circle roots. This must be avoided as a valid inverse cannot be found for an input signal which contains these frequency components. In practice, unit circle roots can occur during design, but can be removed through the addition of a common delay term to all model analysis filters, i.e., a uniform change to the Δ_i delay terms in (2).

While roots of $\det(\mathbf{E}(z))$ on the unit circle can be avoided easily enough, it is entirely unfeasible to insist that all roots remain within the unit circle. As discussed, generally high order and relatively specific FIR analysis filters are used. This leads to a situation where little control exists over the roots of $\det(\mathbf{E}(z))$, and it is thus extremely probable that some roots will naturally fall outside the unit circle.

Since the synthesis filters producing PR will contain poles outside the unit circle, a causal implementation does not exist for them. As sample reconstruction needs to run in real time, anticausal filtering (i.e., a backwards sweep) is not feasible. Practical synthesis filters must be causal and stable. To achieve this, causal FIR reconstruction filters which give an approximate PR solution can be developed. These filters are achieved through a least squares solution to (14).

As $\mathbf{E}(z)$ and $\mathbf{R}(z)$ both contain only FIR elements, they can be written in a convolutional matrix equation in order to find a least squares solution. This is expressed through the matrix equation

$$\mathcal{R}\mathcal{E} = \mathcal{P}, \quad (17)$$

where \mathcal{R} , \mathcal{E} , and \mathcal{P} are large scalar matrices designed so (17) closely approximates (14). This is done through replacing the polynomial elements in (14) as follows. The known polynomial elements of $\mathbf{E}(z)$ are each replaced with size $s \times t$ block

Toeplitz submatrices through

$$\mathbf{E}_{ij}^T = \begin{bmatrix} e_{ij}(0) & 0 & 0 \\ e_{ij}(1) & e_{ij}(0) & \vdots \\ \vdots & e_{ij}(1) & \vdots \\ e_{ij}(n-1) & \vdots & \ddots & 0 \\ 0 & e_{ij}(n-1) & e_{ij}(0) \\ \vdots & 0 & \ddots & e_{ij}(1) \\ \vdots & \vdots & \vdots \\ 0 & 0 & e_{ij}(n-1) \end{bmatrix}, \quad (18)$$

where the component values, $e_{ij}(0), e_{ij}(1), \dots, e_{ij}(n-1)$, are the coefficients of the polynomial $E_{ij}(z)$. Without loss of generality, causal model analysis filters are assumed in this notation. Similarly, the yet unknown polynomial elements of $\mathbf{R}(z)$ are each replaced with length s row vectors,

$$\mathbf{R}_{ij} = [r_{ij}(0) \quad r_{ij}(1) \quad \dots \quad r_{ij}(s-1)]. \quad (19)$$

The terms of $\mathbf{P}(z)$ are replaced with length t row vectors according to

$$\mathbf{P}_{ij} = \begin{cases} [0 \dots 0 & 1 & 0 \dots 0] & \text{for } \mathbf{P}_{ij}(z) = z^{-k} \\ [0 & \dots & 0] & \text{for } \mathbf{P}_{ij}(z) = 0, \end{cases} \quad (20)$$

where the $(k+1)^{th}$ entry is the nonzero entry in the case of $\mathbf{P}_{ij}(z) = z^{-k}$. Note that constant c of (14) has been set equal to one in this representation, corresponding to a unity gain in reconstruction system.

Using the representations (18), (19), and (20) on the $L \times L$ matrices in (14) leads to (17) with known matrices \mathcal{E} of size $sL \times tL$ and \mathcal{P} of size $L \times tL$ and unknown matrix \mathcal{R} of size $L \times sL$. \mathcal{R} is solved through the least squares solution to (17). Its entries have a one-to-one mapping to the synthesis filter coefficients. Thus, a numerical solution for the synthesis filters can be found which is optimal in the least squares sense.

A few comments should be made on this numerical solution. First, while \mathcal{E} is fixed for a specific sampler model, \mathcal{P} can be altered depending on the parameters d' and r of (14). Altering these parameters produces different \mathcal{R} and, while an exhaustive search with simulations can determine the best choice, selection should place $d' \approx t/2$. That is, at approximately half the row length of \mathcal{P} , which allows for a roughly equal number of FIR filter coefficients to approximate both the causal and anticausal portions of the synthesis filters' IIR responses.

The fact that an $(n-1)^{th}$ order polynomial is used in the representation of \mathbf{E}_{ij} should also be mentioned. As the individual entries of $\mathbf{E}(z)$ can (and typically do) differ in order, $n-1$ should be considered the order of the largest polynomial, allowing all \mathbf{E}_{ij} to be of the same size. The higher indexed coefficients of lower order polynomials can be set to zero. This can result in some all zero columns of \mathcal{E} , but these will correspond to all zero columns of \mathcal{P} (provided $d' \approx t/2$) and do not affect the solution. Removing these all zero columns can reduce solution computation time, depending on the numerical algorithm used.

Finally, some comments on the sizes of these matrices will be made. The above solution produces L synthesis filters,

each with sL taps. Naturally, selecting a larger s produces filters with less reconstruction error. As will be shown in Section 5 through some specific design examples, filter coefficient quantization reduces a considerable number of these coefficients to 0. This, along with the fact that the solution can produce many coefficients equal to zero, means that sL is the maximum number of filter coefficients. The actual number can be considerably lower, and simulations illustrate this fact. Finally, increasing s beyond a certain point will not produce a significant increase in performance, especially when filter coefficient quantization is considered as these additional synthesis filter coefficients will be close to zero.

IV. OVERSAMPLING

An accurate reconstruction technique will require some degree of oversampling, or obtaining samples at an average rate faster than the Nyquist rate. This section will differentiate between two types of oversampling. The first type is the classic case, where $T_s < T_N$. This produces a sampled signal, $x[n]$, which has a zero-valued magnitude response in the highpass region, that is frequencies centered about π . This form of oversampling diminishes the effects of inaccuracies in the model interpolation filters of (7). As discussed in the previous section, the inaccuracies of these truncated and windowed fractional delay transfer functions will primarily exist in the high frequencies of the normalized spectrum, about $\omega = \pi$. Sufficiently oversampled signals will therefore not contain any signal components in the portions of the spectrum for which the models are inaccurate. For this type of oversampling, the reconstructed signal $\hat{x}[n]$ will also be oversampled.

The second type of oversampling is produced through use of additional channels in the filter bank, or the case where $L > M$. Since the number of channels is greater than the decimation factor, this case results in what is commonly referred to as a "nonmaximally decimated" filter bank. For this case of oversampling, L samples are periodically extracted every MT_s seconds. Unlike the previous type of oversampling, $\hat{x}[n]$ will not itself be oversampled if $T_s = T_N$. This second type of oversampling is a result of more samplers, whereas the first type is a result of faster samplers. Naturally, both types can be used together.

Using faster samplers has little effect on the numerical solution of the previous section. However, the use of additional samplers allows for some changes in numerical solution, which will now be elaborated upon. The design of the model analysis filters is still performed with (7). However, design of the synthesis filters is subject to a slight change in the polyphase matrix representation resulting from the fact that the number of channels is greater than the decimation factor.

With the orders of the decimation and expansion operations equal to M , and the number of channels equal to L , the filter banks are given by

$$\begin{bmatrix} H_0(z) \\ \vdots \\ H_{L-1}(z) \end{bmatrix} = \mathbf{E}(z^M) \begin{bmatrix} 1 \\ \vdots \\ z^{-(M-1)} \end{bmatrix} \quad (21)$$

where

$$\mathbf{E}(z) = \begin{bmatrix} E_{0,0}(z) & \cdots & E_{0,M-1}(z) \\ \vdots & & \vdots \\ \vdots & & \vdots \\ E_{L-1,0}(z) & \cdots & E_{L-1,M-1}(z) \end{bmatrix} \quad (22)$$

for the analysis bank, and

$$[F_0(z) \quad \cdots \quad F_{L-1}(z)] = [z^{-(M-1)} \quad \cdots \quad 1] \mathbf{R}(z^M), \quad (23)$$

where

$$\mathbf{R}(z) = \begin{bmatrix} R_{0,0}(z) & \cdots & \cdots & R_{0,L-1}(z) \\ \vdots & & & \vdots \\ R_{M-1,0}(z) & \cdots & \cdots & R_{M-1,L-1}(z) \end{bmatrix} \quad (24)$$

for the synthesis bank. A PR condition is again provided by (14). FIR polynomials for (24) yielding PR can be determined by viewing the reconstruction filter bank as a Bezout inverse system [21]. Specifically, provided $\mathbf{E}(z)$ is a delay permissive right coprime matrix, which is generically the case (i.e., with probability one) for $L > M$, then there exists a polynomial matrix $\mathbf{R}(z)$ such that (14) holds. For $\mathbf{E}(z)$ to be delay permissive right coprime, the determinant of its greatest common right divisor must equal dz^{-l} with d constant and l integer. Note that the polynomial matrix $\mathbf{R}(z)$ in (14) is not unique, and a procedure for constructing a solution of minimal order is described in [22]. It is worth noting that when the order of $\mathbf{E}(z)$ is large, the order of $\mathbf{R}(z)$ is also large, in which case a least squares approximation similar to the one employed in Section III-B may still be needed.

As in the least squares convolutional matrix solution, a Bezout inverse solution is determined through representation of (14) in terms of large scalar matrices. Representing $\mathbf{E}(z)$ as the sum of delay weighted coefficient matrices,

$$\mathbf{E}(z) = \mathbf{E}_0 + z^{-1}\mathbf{E}_1 + \cdots + z^{-(n-1)}\mathbf{E}_{n-1}, \quad (25)$$

where $n-1$ here is the maximum order of all its polynomial elements, allows a scalar block Toeplitz matrix to be formed,

$$\mathcal{E} = \begin{bmatrix} \mathbf{E}_{n-1} & \mathbf{E}_{n-2} & \cdots & \mathbf{E}_0 & \mathbf{0} & \cdots & \mathbf{0} \\ \mathbf{0} & \mathbf{E}_{n-1} & \mathbf{E}_{n-2} & \cdots & \mathbf{E}_0 & \cdots & \mathbf{0} \\ \vdots & \ddots & \ddots & & & \ddots & \vdots \\ \mathbf{0} & \cdots & \mathbf{0} & \mathbf{E}_{n-1} & \mathbf{E}_{n-2} & \cdots & \mathbf{E}_0 \end{bmatrix}. \quad (26)$$

This matrix consists of m block rows and $m+n-1$ block columns. Also representing $\mathbf{R}(z)$ as the sum of delay weighted coefficient matrices,

$$\mathbf{R}(z) = \mathbf{R}_0 + z^{-1}\mathbf{R}_1 + \cdots + z^{-(m-1)}\mathbf{R}_{m-1}, \quad (27)$$

where $m-1$ is the maximum order of its polynomial elements, allows for a corresponding block vector,

$$\mathcal{R} = [\mathbf{R}_{m-1} \quad \cdots \quad \mathbf{R}_0]. \quad (28)$$

Likewise, the delay weighted coefficient matrix representation of

$$\mathbf{P}(z) = \mathbf{P}_0 + z^{-1}\mathbf{P}_1 + \cdots + z^{-(m+n-1)}\mathbf{P}_{m+n-1}, \quad (29)$$

allows for the block vector

$$\mathcal{P} = [\mathbf{P}_{m+n-1} \quad \cdots \quad \mathbf{P}_0]. \quad (30)$$

The blocks of \mathcal{P} are of size $M \times M$, and most are equal to $\mathbf{0}$. The procedure of [22] is used to determine the solution as well as to find the order $m-1$.

While oversampling through additional channels allows FIR synthesis filters that achieve PR to be found, it is not always desirable to use such a precise solution. As the analysis bank model contains some error over the entire spectrum (albeit small if well designed), a PR solution corrects for this error. Since the actual sampled signal does not contain such error, the finely tuned reconstruction filters correct for signal distortion that does not exist. A lower order approximate PR solution does not correct for the extremely fine model distortions. Because of this, a lower order approximate PR solution can sometimes perform better than a high order PR solution.

V. DESIGN EXAMPLES AND SIMULATION RESULTS

This section presents some reconstruction filter bank design examples with simulation results for the applications of bunched sampling and time-interleaved ADCs described in Section II. The design techniques of Sections III and IV were used.

Overall system performance is dependent on two factors: the precision of signal modelling through the analysis bank, and the precision of signal reconstruction through the synthesis bank. The effects can be examined separately. Synthesis filters can be designed that produce a PR or near PR system, but if the analysis filter modelling was inaccurate the reconstructed signal will contain significant errors. For this reason, a PR system and perfect signal reconstruction are not synonymous.

Since the analysis filters serve only to model the nonuniformly sampled signal and are not implemented, there are no direct implementation concerns. Thus, very high order analysis filters are attractive for signal modelling. High order synthesis filters are also desirable from a performance standpoint, but not in terms of implementation cost. In order to achieve a close approximation to a perfect reconstruction system, the orders of the synthesis filters will increase as the orders of the analysis filters increase. Thus, analysis filters of too high an order create an undesirably costly synthesis bank. Likewise, high order synthesis filters will not perform well if the analysis filters are of too low an order.

Overall reconstruction performance is evaluated through examining the signal-to-error ratio over N uniform samples,

$$SER = 10 \log_{10} \left(\frac{\sum_{n=0}^{N-1} |x[n]|^2}{\sum_{n=0}^{N-1} |x[n] - \hat{x}[n + d_t]|^2} \right), \quad (31)$$

where d_t is the total delay imposed by the reconstruction system. Using bandlimited noise as a test signal allows for performance evaluation up to a chosen fraction of the theoretically maximum bandwidth that the system is capable of reconstructing. Varying the test signal bandwidth is an effective method of determining the frequency range that is accurately modelled by the analysis bank (or equivalently, the ratio of oversampling necessary for a desired level of performance).

A. Bunched Sampling and Reconstruction Filter Quantization

A case of bunched sampling was presented in [15], using an alternate approach for analysis filter modelling, which produces the same reconstruction system as the method presented in this paper. In this design example, samples are taken in periodic bunches of 5, with intervals of $5T_s$ between the first samples of consecutive bunches and intervals of $T_s/2$ between consecutive samples within a bunch. T_s is the uniform sampling period of the reconstructed signal, $\hat{x}[n]$, and the average sampling period of the bunched sampling process. For this sampling process, the reconstruction filter bank will be maximally decimated and have 5 channels ($L = M = 5$). Using (4), the ideal model analysis filters are given by

$$H_n(e^{j\omega}) = e^{-j\omega 0.5n}, \quad (32)$$

for $n = 0, 1, \dots, 4$. The equivalent ideal time-domain responses of (5) produce even indexed analysis filters which are simple one-tap delays. Thus, truncation and windowing only affects the odd indexed analysis filters.

In the results presented, the analysis filters are truncated to 76 taps and a Kaiser window is used with shape parameter $\beta = 10$ to smooth the responses. 80th order reconstruction filters were developed using the least squares method of (17). The magnitude responses of the reconstruction filters are shown in Fig. 5. The fact that the analysis and synthesis filters were of relatively high order made the approximation to a PR filter bank very accurate. Although not shown here, the magnitude responses of the alias component transfer functions were all on the order of 10^{-13} over the entire normalized spectrum, and error in the distortion transfer function, $\hat{X}(e^{j\omega})/X(e^{j\omega})$, was of similar order. This indicates an improvement in performance over a previous reconstruction method presented in [7], which did not allow the alias component transfer function to be directly controlled.

Using bandlimited noise as an input signal, the SER results of Fig. 6 are obtained with $N = 2000$. Curves are shown for both 16-bit quantized and unquantized reconstruction filter coefficients. Each data point indicates the SER performance for a signal bandlimited to the indicated fraction of theoretical maximum bandwidth. Performance is good for frequencies up to about 90% of the theoretical maximum bandwidth. The loss of performance at the upper edge of the frequency band is a result of the inaccuracies of the model analysis filters due to the transition band resulting from the windowing process. Decreasing the width of the transition band results in increased ripples in the models which degrade the performance. Quantization introduces an effective floor to the SER performance in Fig. 6 at approximately 65dB. For a desired level of quantization, the transition band should be decreased in width until the resulting SER would fall below the SER floor due to quantization.

A more detailed examination of the effects of quantization is shown in Fig. 7. Here, the SER of an input signal occupying 90% of the theoretical maximum bandwidth (i.e., 90% of the Nyquist frequency) is determined for varying levels of reconstruction filter quantization. All other conditions above remain unchanged. The SER result for unquantized coefficients is shown as an upper boundary to SER performance.

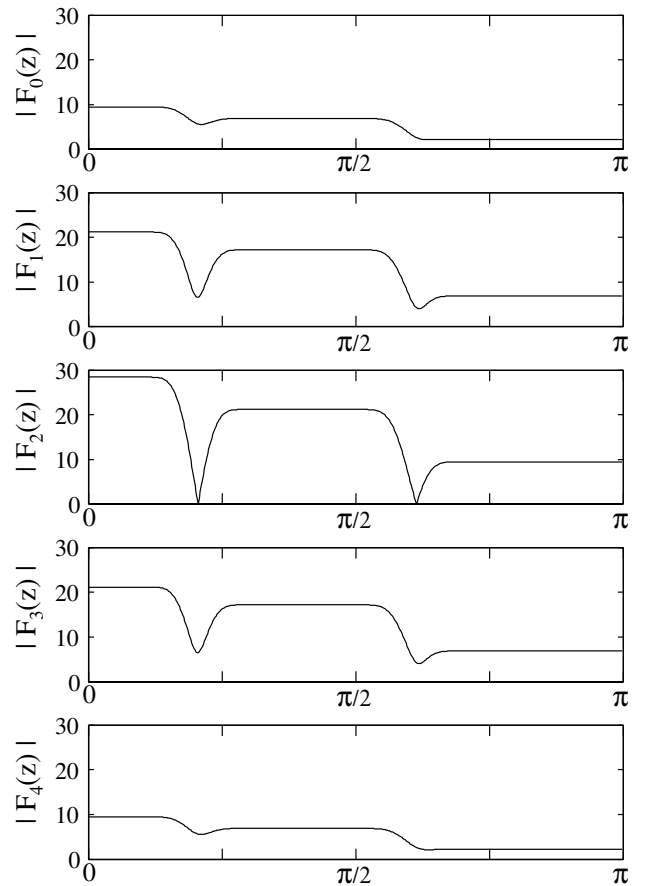


Fig. 5. Magnitude responses of the synthesis filters for the example of Section V-A.

The performance as a function of synthesis filter size is shown in Fig. 8 for quantized and unquantized coefficients. Again, an input signal occupying 90% of the theoretical maximum bandwidth was used. Quantization limits the performance capabilities, as is demonstrated here for the case of 16-bit coefficients. For this particular case of bunched sampling, increasing the synthesis filters' order above 80 did not increase performance. In this simulation, model analysis filters closely matching (32) were used to produce the results. It was found that introducing common time shifts to these model filters resulted in significantly higher order reconstruction filters (more than double the complexity) in order to achieve similar levels of performance. This is a direct result from the fact that the time shift results in fewer delays which are perfectly modelled using a single tap filter.

B. Oversampling Performance

Reconstruction performance was evaluated for the case of oversampling by way of additional filter bank channels, as discussed in Section IV. Again, a bunched sampling process is examined. As in the previous example, periodic bunches of 5 samples are taken. However, the interval between the first samples of consecutive bunches is $3T_s$, and the interval between consecutive samples in a bunch is $3T_s/10$. This results in a five channel nonmaximally decimated filter bank

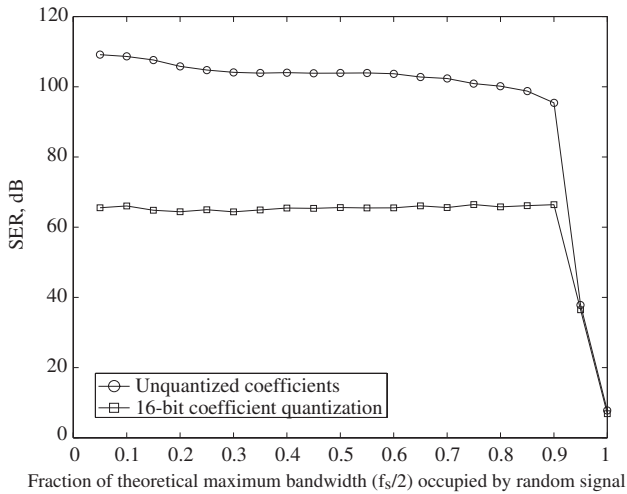


Fig. 6. SER as defined in (31) vs. input signal bandwidth for a random bandlimited input signal for the example of Section V-A. Results for quantized (16-bits) and unquantized filter coefficients shown.

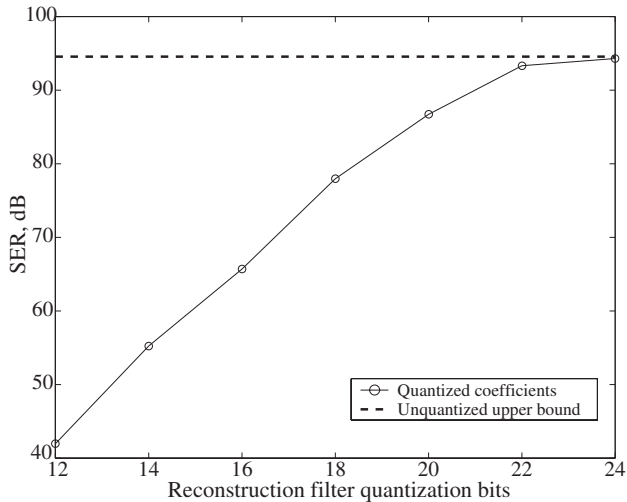


Fig. 7. SER for an input signal occupying 90% of the theoretical maximum bandwidth as a function of reconstruction filter quantization. Unquantized upper bound shown (dashed).

with a decimation factor of 3 ($L = 5, M = 3$). Through (4), the ideal model analysis filters are equal to

$$H_n(e^{j\omega}) = e^{-j\omega 0.3n}, \quad (33)$$

for $n = 0, 1, \dots, 4$. The spacing of the samples in this example is such that only one analysis filter ($H_0(e^{j\omega})$ in this case) can have a trivial single tap response.

Three reconstruction filter banks (composed of 5 filters each) were designed. The first was designed via the Bezout inverse method to design 113th order filters. Because of the high order of the model analysis polyphase matrix of (22) (containing components of 25th order), the synthesis filters are actually the minimal order solution. The second and third banks of reconstruction filters were designed using the least squares method to achieve 113th order and 55th order synthesis filters.

The performance of these three reconstruction filter banks is

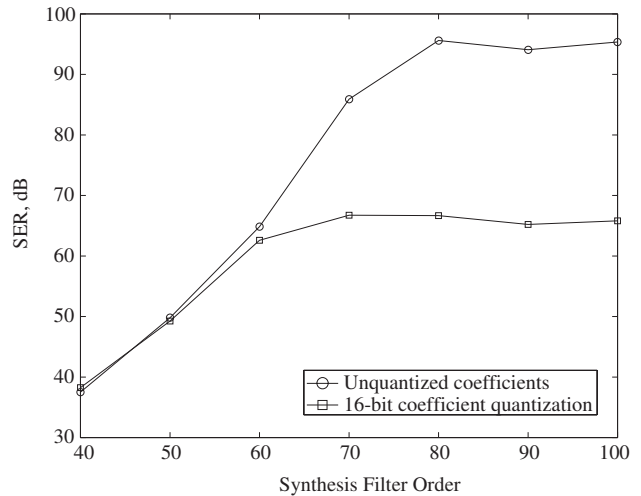


Fig. 8. SER for an input signal occupying 90% of the theoretical maximum bandwidth as a function of reconstruction filter size.

shown in Fig. 9. The higher order filters designed through the least squares and Bezout inverse methods have nearly identical performance. This is not surprising, as the methods' respective filters (not depicted here) have nearly identical responses, with any differences resulting from the algorithm used to find a numerical inverse. Interestingly, the lower order filter bank designed through the least squares method has performance superior to the higher order filters. This can be accounted for as an effect of the inaccuracy of the model analysis filters. While the methods designing higher order synthesis filters form a PR system, they do so only for the model, not the actual sampling process. A lower order reconstruction filter bank, while less precise according to the model, can be more precise with respect to the actual system. The reconstruction filter bank performance for this particular case of oversampling is quite good, with an SER over 100dB for signals bandlimited to 90% of the theoretical maximum bandwidth. Performance at this high level is generally possible for oversampled cases provided samples are not too close to overlapping.

C. Interleaved ADC Performance

For the interleaved ADC case, an example from [9] will be used. The continuous-time signal, $x(t)$, is composed of the sum of four sinusoid terms with unit amplitude and respective frequencies of $f_s/16$, $f_s/8$, $3f_s/16$, and $f_s/4$. For each sinusoid, a random phase with uniform distribution from 0 to 2π was used. Five interleaved ADCs with respective Δ_i offsets $[0, 0.96T_s, 2.02T_s, 2.99T_s, 4.03T_s]$ were modelled. This corresponds to respective sample-time errors of $[0, -0.04T_s, 0.02T_s, -0.01T_s, 0.03T_s]$. Analyzing the sampled signal as though it were sampled without timing error (i.e., uncorrected) results in the magnitude plot of Fig. 10(a). The 4 tones extending to 0dB are the only desired tones, all others have resulted from the imperfect sampling and are undesired. Application of reconstruction filters designed through the least squares method produces the recovered sequence $\hat{x}[n]$, which has the magnitude spectrum shown in Fig. 10(b). The SER of $\hat{x}[n]$ obtained through (31) is approximately 99dB

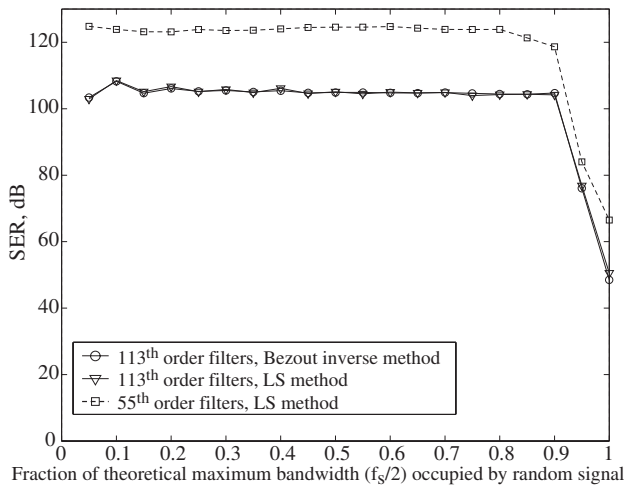


Fig. 9. SER vs. input signal bandwidth for an oversampled bandlimited random signal. Results show performance of filter banks of various orders designed through the Bezout inverse and least squares methods.

over $N = 2000$ samples. The reconstruction filters are 149^{th} order, but truncation and coefficient quantization as in Section V-A will reduce the number of nonzero coefficients.

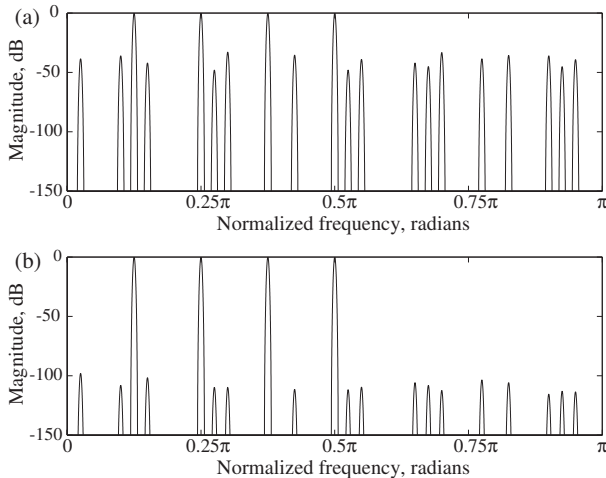


Fig. 10. Magnitude spectral plots of (a) sequence obtained through interleaved samplers with sample-time errors and (b) reconstructed sequence, $\hat{x}[n]$.

The magnitude spectrum of the reconstructed signal presented in this paper is comparable to the results obtained in [9]. Through this paper's methods, the magnitude of the undesired tones can be reduced further than shown in Fig. 10(b), but would require implementation of significantly higher order and very precise synthesis filters. The gain in performance obtained would probably not justify the increased cost of implementation.

The method of [9] has some key advantages in implementation. Through use of Farrow structured [23] synthesis filters, the reconstruction process can be adapted for varying interleaved timing errors, a critical feature for interleaved ADCs, where timing error is unintentional and must be measured. An advantage of this paper's technique is that it allows for a greater range of input signal frequencies, relative to the

average sampling rate. As [9] relies on a PR condition that is only valid over certain spectral regions, $x(t)$ is bandwidth bound to a smaller fraction of the average sampling frequency than the method of this paper. As discussed in Section V-A, this paper's technique provides good reconstruction for most of the range of frequencies from dc to half the average sampling rate, with degradation in performance over a small band due to modelling inaccuracies.

VI. CONCLUSION

This paper has described a new technique for reconstruction of a bandlimited signal from its periodic nonuniform samples. Using a model for the nonuniform sampling process, reconstruction was viewed in terms of a perfect reconstruction multirate filter bank problem. A method approximating perfect reconstruction conditions was used to determine FIR filters that obtain a uniformly sampled output with negligible distortions and negligible transfer of alias components. The presented design examples and simulation results for various cases show this paper's methods do produce an implementable filter bank recovering uniform samples with low error.

REFERENCES

- [1] H. Nyquist, "Certain Topics in Telegraph Transmission Theory," *AIEE Trans.*, pp. 617-644, 1928.
- [2] C. E. Shannon, "Communication in the presence of noise," *Proc. IRE*, vol. 37, pp. 10-21, Jan. 1949.
- [3] J. L. Yen, "On nonuniform sampling of bandwidth-limited signals," *IRE Trans. Circuit Theory*, vol. CT-3, pp. 251-257, Dec. 1956.
- [4] A. Papoulis, "Generalized sampling expansion," *IEEE Trans. Circuits Systems*, vol. CAS-24, pp. 652-654, Nov. 1977.
- [5] J. L. Brown, Jr., "Multi-channel sampling of low-pass signals," *IEEE Trans. Circuits Systems*, vol. CAS-28, pp. 101-106, Feb. 1981.
- [6] P. P. Vaidyanathan, V. C. Liu, "Classical sampling theorems in the context of multirate and polyphase digital filter bank structures," *IEEE Trans. Acoust., Speech, Signal Processing*, vol. 36, pp. 1480-1495, Sept. 1988.
- [7] P. P. Vaidyanathan, V. C. Liu, "Efficient reconstruction of band-limited sequences from nonuniformly decimated versions by use of polyphase filter banks," *IEEE Trans. Acoust., Speech, Signal Processing*, vol. 38, pp. 1927-1936, Nov. 1990.
- [8] Y. C. Eldar, A. V. Oppenheim, "Filterbank reconstruction of bandlimited signals from nonuniform and generalized samples," *IEEE Trans. Sig. Proc.*, vol. 48, pp. 2864-2875, Oct. 2000.
- [9] H. Johansson, P. Löwenborg, "Reconstruction of nonuniformly sampled bandlimited signals by means of digital fractional delay filters," *IEEE Trans. Sig. Proc.*, vol. 50, pp. 2757-2767, Nov. 2002.
- [10] W. Namgoong, "Finite-Length Synthesis Filters for Non-Uniformly Time-Interleaved Analog-to-Digital Converter," *IEEE Int. Symposium on Circuits and Systems*, vol. 4, pp. 815-818, May 2002.
- [11] R. Venkataramani, Y. Bresler, "Perfect reconstruction formulas and bounds on aliasing error in sub-Nyquist nonuniform sampling of multiband signal," *IEEE Trans. Info. Theory*, vol. 46, pp. 2173-2183, Sept. 2000.
- [12] R. Venkataramani, Y. Bresler, "Optimal sub-Nyquist nonuniform sampling and reconstruction for multiband signals," *IEEE Trans. Sig. Proc.*, vol. 49, pp. 2301-2313, Oct. 2001.
- [13] Y. -C. Jenq, "Perfect reconstruction of digital spectrum from nonuniformly sampled signals," in *Proc. Instrumentation and Measurement Technology Conference*, Ottawa, Ont., vol. 1, pp. 624-627, 1997.
- [14] F. Marvasti, *Nonuniform Sampling, Theory and Practice*. Kluwer, 2001.
- [15] R. S. Prendergast, B. C. Levy, and P. J. Hurst, "Multirate filter bank reconstruction of bandlimited signals from bunched samples," in *Proc. 36th Asilomar Conference on Signals, Systems, and Computers*, Pacific Grove, CA, vol. 1, pp. 781-785, Nov. 2002.
- [16] X. Aragones, J.L. Gonzalez, and A. Rubio, *Analysis and Solutions for Switching Noise Coupling in Mixed-Signal ICs*. Kluwer, 1999.
- [17] S. Donnay and G. Gielen, Ed., *Substrate Noise Coupling in Mixed-Signal ASICs*. Kluwer, 2003.

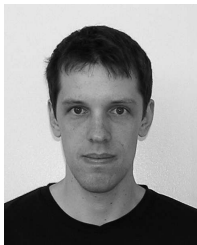
- [18] A. V. Oppenheim, R. W. Schaffer, with J. R. Buck, *Discrete-Time Signal Processing*. Upper Saddle River, NJ: Prentice-Hall, 1999.
- [19] T. I. Laakso, V. Välimäki, M. Karjalainen, and U. K. Laine, "Splitting the Unit Delay," *IEEE Sig. Proc. Magazine*, vol. 13, no. 1, January 1996, pp. 30-60.
- [20] P. P. Vaidyanathan, *Multirate Systems and Filter Banks*. Englewood-Cliffs, NJ: Prentice-Hall, 1993.
- [21] T. Kailath, *Linear Systems*. Englewood-Cliffs, NJ: Prentice-Hall, 1980.
- [22] R. R. Bitmead, S.-Y. Kung, B. D. O. Anderson, and T. Kailath, "Greatest common divisors via generalized Sylvester and Bezout matrices," *IEEE Trans. Automat. Contr.*, vol. AC-23, no. 6, pp. 1043-1047, Dec. 1978.
- [23] C. W. Farrow, "A continuously variable digital delay element," *IEEE Inter. Symp. Circuits Systems*, June 7-9, 1988, vol. 3, pp. 2641-2645.



Paul J. Hurst (S'76-M'83-SM'94-F'01) received the B.S., M.S., and Ph.D. degrees in electrical engineering from the University of California at Berkeley in 1977, 1979, and 1983, respectively.

From 1983 to 1984, he was with the University of California, Berkeley, as a lecturer, teaching integrated-circuit design courses and working on an MOS delta-sigma modulator. In 1984, he joined the telecommunications design group of Silicon Systems Inc., Nevada City, CA, where he was involved in the design of CMOS integrated circuits for voice-band modems. Since 1986, he has been on the faculty of the Department of Electrical and Computer Engineering at the University of California at Davis, where he is now a Professor. His research interests are in the areas of data converters and analog and mixed-signal integrated-circuit design for digital communications.

Professor Hurst has served on the program committees for the Symposium on VLSI Circuits and the International Solid-State Circuits Conference. He was a guest editor for the December 1999 issue of the *Journal of Solid-State Circuits*. He is now an associate editor for the *Journal of Solid-State Circuits*. He is a co-author of a textbook on analog integrated-circuit design. He is also active as a consultant to industry.



Ryan S. Prendergast (S'02) was born in California in 1979. He received his B.S. and M.S. degrees in Electrical Engineering from the University of California at Davis in 2001 and 2003, respectively. He is currently pursuing his Ph.D. at the University of California, San Diego.

His research interests are in the areas of sampling theory and multirate digital signal processing.



Bernard C. Levy (F'94) received the diploma of Ingénieur Civil des Mines from the Ecole Nationale Supérieure des Mines in Paris, France, and the Ph.D. in Electrical Engineering from Stanford University.

From July 1979 to June 1987 he was Assistant and then Associate Professor in the Department of Electrical Engineering and Computer Science at M.I.T. Since July 1987, he has been with the University of California at Davis, where he is Professor of Electrical Engineering and a member of the Graduate Group in Applied Mathematics. He served as Chair

of the Department of Electrical and Computer Engineering at UC Davis from 1996 to 2000. He was a Visiting Scientist at the Institut de Recherche en Informatique et Systèmes Aléatoires (IRISA) in Rennes, France from January to July 1993, and at the Institut National de Recherche en Informatique et Automatique (INRIA), in Rocquencourt, France, from September to December 2001. His research interests are in statistical signal processing, estimation, detection, and multidimensional signal processing.

He currently serves as Associate Editor of the *IEEE Transactions on Circuits and Systems II* and served as a member of the Image and Multidimensional Signal Processing technical committee of the IEEE Signal Processing Society from 1992 to 1998. He is a member of SIAM and the Acoustical Society of America.